Korean Journal of Geomatics
Vol. 3, No. 1 / June 2003
pp. 53~57

A Study on the Analysis of Geometric Accuracy of Tilting Angle Using KOMPSAT-1 EOC Images

Doo-Chun SEO* and Hyo-Suk LIM**

Abstract

As the Korea Multi-Purpose Satellite-1 (KOMPSAT-1) satellite can roll tilt up to ±45°, we have analyzed some KOMPSAT-1 EOC images taken at different tilt angles for this study. The required ground coordinates for bundle adjustment and geometric accuracy are obtained from the digital map produced by the National Geography Institution, at a scale of 1:5,000. Followings are the steps taken for the tilting angle of KOMPSAT-1 to be present in the evaluation of geometric accuracy of each different stereo image data: Firstly, as the tilting angle is different in each image, the characteristic of satellite dynamic must be determined by the sensor modeling. Then the best sensor modeling equation should be determined. The result of this research, the difference between the RMSE values of individual stereo images is mainly due to quality of image and ground coordinates instead of tilt angle. The bundle adjustment using three KOMPSAT-1 stereo pairs, first degree of polynomials for modeling the satellite position, were sufficient.

Keywords : *Tilt angle, KOMPSAT-1 EOC, Position Accuracy, Bundle Adjustment*

1. Introduction

Korea Multi-Purpose Sarellite-1(KOMPSAT-1) was successfully launched in 1999 and Korea became one of the countries in the world to have their own earth observation satellites. KOMPSAT-1 is designed for multiple missions to provide various applications in the field of earth observation covering land and ocean. Its main mission is the production of cartographic maps of Korea. Images are collected and processed to support the development of maps of Korean Peninsula. The EOC is KOMPSAT-1's main payload for the purpose of cartography to produce digital map of Korea.

In this paper, we analyzed the geometric accuracy of KOMPSAT-1 EOC image, whose tilting angles are variable. As the KOMPSAT-1 can roll tilt up to ±45°, we have analyzed some EOC images taken at three different tilt angles(5°, 15°, 27°) for this study. The required ground coordinates for bundle adjustment and geometric accuracy are obtained from the digital map produced by the National Geography Institution, at a scale of 1:5,000 and the image coordinates are read with the sub-pixel accuracy.

These are the steps taken for the tilting angle of KOMPSAT-1 for the evaluation of the accuracy of geometric accuracy of each different stereo image data: Firstly, as the tilting angle is different in each image, the satellite dynamic characteristic must be determined sensor modeling, and the best sensor modeling equation is determined. Then the control points (from the sensor modeling equation) are evaluated by calculating of the covariance matrix (σ_X, σ_Y, σ_{XY}, σ_Z) and image coordinates' residual (V_X, V_Y) related to the ground coordinates. Finally, the check points are evaluated through RMSE's coordinate of check points, which were calculated from sensor modeling.

2. Bundle Adjustment for Linear Array CCD Sensor

The image data used in this work is collected as follows. The satellite moves along a well defined close-

*Senior Researcher, Satellite Operation & Application Center, Korea Aerospace Research Institut (E-mail : dcivil@kari.re.kr)
**Senior Researcher, Satellite Operation & Application Center, Korea Aerospace Research Institut (E-mail : hsliml@kari.re.kr)

The manuscript for this paper was received on June 25, 2003 / accepted on June 30, 2003.

to-circular elliptical orbit. Along track the sensor is always pointing to the center of the earth. The images are taken with pushbroom type sensor at constant time interval. The images have a cylindrical perspective, usually distorted due to attitude variations. A single image consists of a fixed number of consecutive scan lines. Each line has its own time-dependent position and attitude parameters. These exterior orientations are represented by 6 parameters. (3 parameters; position, 3 parameters; attitude) Because these position and attitude parameters are correlated, one parameter can be fixed for processing.

The applied bundle adjustment utilized the orbital geometry in which orbital parameters are used to determine the satellite position and orientation with respect to the ground coordinates system at any time.

The actual position $S(X_S, Y_S, Z_S)$ of the satellite at a given time, deviates from the nominal position $S(X_S', Y_S', Z_S')$. These deviations are modeled as time polynomials to be included in the mathematical model for actual satellite positions and orientation. The actual satellite position can be calculated as follows:

$$\begin{bmatrix} X_s \\ Y_s \\ Z_s \end{bmatrix} = \begin{bmatrix} X_s' \\ Y_s' \\ Z_s' \end{bmatrix} + \begin{bmatrix} \Delta X \\ \Delta Y \\ \Delta Z \end{bmatrix} = M_b^T \begin{bmatrix} 0 \\ 0 \\ R_{s'} \end{bmatrix} + \begin{bmatrix} \Delta X \\ \Delta Y \\ \Delta Z \end{bmatrix} \quad (1)$$

M_b and $R_{s'}$ can be calculated from the Eulerian parameters, which are also estimated using the ephemeris data. To determine the satellite orientation, the rotation matrix M_b is multiplied by another rotation matrix M_a. The M_a will take care of angular deviations caused by the various unknown forces and the ellipsoidal figure of the earth. $R_{s'}$ is the distance from the earth center to the nominal satellite position.

We can write the following set of collinearity equation for any point vector:

$$M_T \begin{bmatrix} x' \\ y' \\ z' \end{bmatrix} = k M_a M_b \left[\begin{bmatrix} X \\ Y \\ Z \end{bmatrix} - M_b^T \begin{bmatrix} 0 \\ 0 \\ R_{s'} \end{bmatrix} - \begin{bmatrix} \Delta X \\ \Delta Y \\ \Delta Z \end{bmatrix} \right] \quad (2)$$

where, M_T is tilt angle, the position deviation vector along the $\Delta X, \Delta Y, \Delta Z$ direction are given by;

$$\begin{aligned} \Delta X &= \delta X_0 + \delta X_1 \Delta t + \delta X_2 \Delta t^2 \\ \Delta Y &= \delta Y_0 + \delta Y_1 \Delta t + \delta Y_2 \Delta t^2 \\ \Delta Z &= \delta Z_0 + \delta Z_1 \Delta t + \delta Z_2 \Delta t^2 \end{aligned} \quad (3)$$

where:

Δt ; the time interval referenced to image frame center

ΔX ; the total position deviation along the X-axis at time Δt

ΔY ; the total position deviation along the Y-axis at time Δt

ΔZ ; the total position deviation along the Z-axis at time Δt

δX_i; i=0,1,2 are the polynomial coefficients of ΔX

δY_i; i=0,1,2 are the polynomial coefficients of ΔY

δZ_i ; i=0,1,2 are the polynomial coefficients of ΔZ

The angular deviation around the three axes are modeled as time polynomial function similarly to that of above. The following is the evaluation of these angular deviations;

$$\begin{aligned} \Delta\omega &= \Delta\omega_0 + \Delta\omega_1 \Delta t + \Delta\omega_2 \Delta t^2 \\ \Delta\phi &= \Delta\phi_0 + \Delta\phi_1 \Delta t + \Delta\phi_2 \Delta t^2 \\ \Delta x &= \Delta x_0 + \Delta x_1 \Delta t + \Delta x_2 \Delta t^2 \end{aligned} \quad (4)$$

where,

Δt ; the time referenced to image center

$\Delta\omega$; the total angular-deviation(Roll) around the

Table 1. Specifications of the three stereo images.

Pre-processing	Level 1R	Level 1R	Level 1R	Level 1R	Level 1R	Level 1R
Scene Center Time	2001-04-08	2000-03-01	2001-11-27	2001-09-10	2000-03-09	2001-10-25
GRS K	927	928	927	927	928	927
GRS J	1324	1325	1334	1334	1334	1334
Orbit Number	6920	1032	10327	9186	1149	9844
Look Angle(deg.)	-6.86	4	-15.29	15.25	-25.91	27.38
Orientation Angle (deg.)	10.01	10.02	-9.57	-14.37	10.16	-15.82
Solar Azimuth (deg.)	138.78	143.72	160.51	138.86	147.81	151.14
Solar Elevation (deg.)	54.22	39.03	29.06	50.52	43.04	35.82
Area	Daejeon		Seoul		Seoul	
Name	Daejeon I		Seoul I		Seoul II	

X-axis at time Δt

$\Delta\phi$; the total angular-deviation(Roll) around the Y-axis at time Δt

Δx ; the total angular-deviation(Roll) around the Z-axis at time Δt

$\delta\omega_i$; i=0,1,2 are the polynomial coefficients of $\Delta\omega$

$\delta\phi_i$; i=0,1,2 are the polynomial coefficients of $\Delta\phi$

δx_i ; i=0,1,2 are the polynomial coefficients of Δx

3. Data and Study Area

The EOC data used in this study includes three stereo images of KOMPSAT-1 digital images. We tested the KOMPSAT-1 tilting capability. A stereo image in Daejeon area and two stereo images in Seoul area are used.

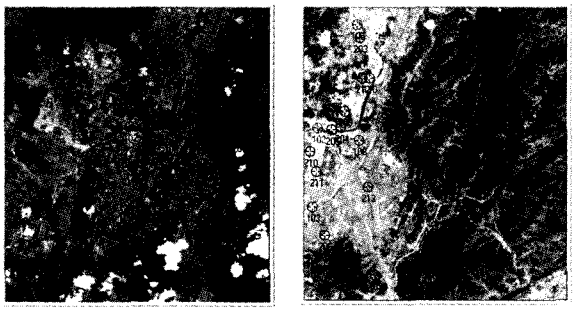

Fig. 1. KOMPSAT-1 EOC Stereo images.
(Red color ; GCPs, Blue color ; CKPs,)

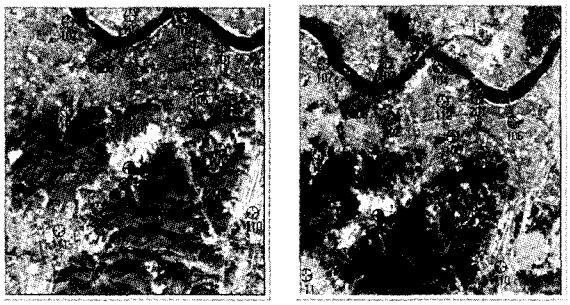

Fig. 2. KOMPSAT-1 EOC Stereo images.
(Red color ; GCPs, Blue color ; CKPs,)

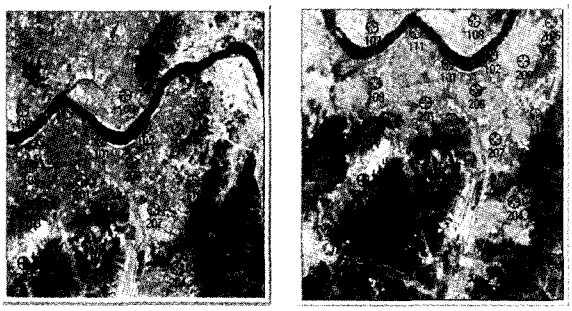

Fig. 3. KOMPSAT-1 EOC Stereo images.
(Red color ; GCPs, Blue color ; CKPs,)

These are level 1A images with ephemeris and attitude data recorded in panchromatic mode. At this level, only detector normalization occurred, without geometric correction for earth curvature or viewing angle effects.

These stereo images are shown in Fig. 1, Fig. 2 and Fig. 3. This area contains cities, mountains and plains where the elevation ranges from 0 to about 700 m.

In order to apply bundle adjustment and verify the model fidelity, the 12 ground control points(GCPs) and about 10 check points(CKPs) distributed around the entire stereo image were selected. The 3D ground coordinates of GCPs and CKPs were captured by a CAD system from a 1:5,000-scale national digital maps in 1995. These captured rectangular planimetric coordinates and height on a geoid were transformed to the Earth-fixed Cartesian coordinates of the World Geodetic System 1984(WGS84) using the Bursa-Wolf model of 7-parameters and the EGM96 model.

The left image coordinates for GCPs and CKPs were determined from magnified images using ERDAS IMAGINE software system. The right image coordinates for GCPs and CKPs were determined using a GCP matching tool from the ERDAS IMAGINE software system. The test images, 12 GCPs marked with triangles and about 10 CKPs marked with circles, are shown in Fig. 1, Fig. 2 and Fig. 3.

4. Experiments and Results

These are the steps taken for the tilting angle of KOMPSAT-1 for the evaluation of geometric accuracy of each different stereo image data: Firstly, as the tilting angle is different in each image, the characteristic of satellite dynamic must be determined by sensor modeling and the best sensor modeling equation can be determined. Then the control points (from the sensor modeling equation) are evaluated by the calculation of covariance matrix (σ_X, σ_Y, σ_{XY}, σ_Z) and image coordinates' residual (V_X, V_Y) related to the ground coordinates.

Finally, the check points are evaluated through RMSE's coordinate of the check points, which were calculated from the sensor modeling.

Several experiments were tested to investigate the performance of polynomial orders as a function of the satellite position deviations or angular deviations of Eq.(3) or (4). 12 GCPs and about 10 CKPs distributed

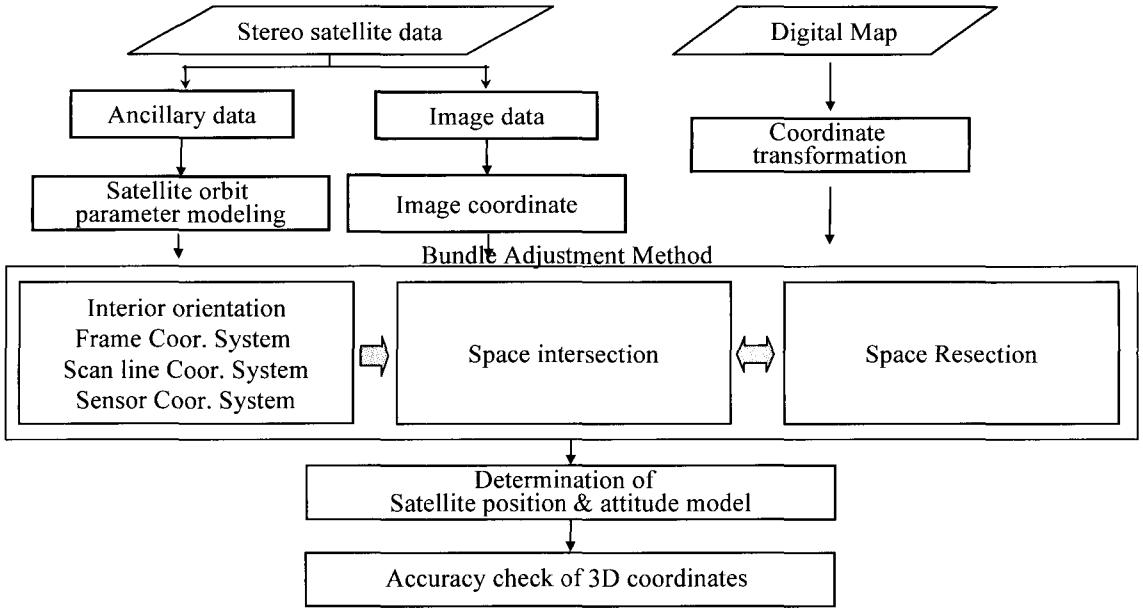

Fig. 4. Flow Chart of Data processing.

around the entire stereo full scenes were used for tests of different orders for $\Delta X, \Delta Y, \Delta Z$ and $\Delta\omega, \Delta\phi, \Delta x$.

5. Discussion

The RMSEs of Table 2, Table 3 and Table 4 provide some information on the differences between the function of polynomial order for the satellite position deviations and angular deviations.

These three experiments are repeated at three different tilt angles(5°, 15° and 25°) and the results are shown in Table 2, Table 3 and Table 4. Generally,

Table 2. The bundle adjustment results of Image 1(Look angle: Left=-6.9 deg., Right=4.0 deg.) (Unit: m)

Case	Position	Attitude			Iter.	Covariance				Residual		RMSE
	X,Y,Z	ω	ϕ	κ		σ_X	σ_Y	σ_{XY}	σ_Z	V_X	V_Y	XYZ
I	1st	1st	1st	1st	12	0.94	0.945	0.942	0.943	0.006	0.008	4.523
II	1st	2nd	2nd	2nd	8	0.659	0.663	0.661	0.661	0.006	0.003	3.207
III	2nd	2nd	2nd	2nd	diver-gence	1.338	1.345	1.342	1.348	0.005	0.008	4.668
IV	1st	Ct	1st	1st	7	0.652	0.655	0.653	0.653	0.006	0.004	3.282
V	1st	Ct	Ct	1st	7	0.612	0.616	0.614	0.614	0.006	0.004	3.225
VI	1st	Ct	Ct	2nd	8	0.674	0.678	0.676	0.677	0.007	0.004	3.282
VII	1st	Ct	Ct	Ct	7	0.629	0.632	0.631	0.631	0.007	0.004	3.196

Table 3. The bundle adjustment results of Image 2(Look angle: Left=-15.3 deg., Right=15.2 deg.) (Unit: m)

Case	Position	Attitude			Iter.	Covariance				Residual		RMSE
	X,Y,Z	ω	ϕ	κ		σ_X	σ_Y	σ_{XY}	σ_Z	V_X	V_Y	XYZ
I	1st	1st	1st	1st	16	8.4	8.434	8.417	8.411	0.018	0.036	4.712
II	1st	2nd	2nd	2nd	11	9.674	9.713	9.693	9.697	0.019	0.034	4.781
III	2nd	2nd	2nd	2nd	12	11.579	11.609	11.594	11.605	0.018	0.031	13.201
IV	1st	Ct	1st	1st	17	9.085	8.991	9.038	8.788	0.029	0.042	5.412
V	1st	Ct	Ct	1st	9	8.09	8.129	8.11	8.103	0.029	0.037	4.695
VI	1st	Ct	Ct	2nd	10	8.131	8.169	8.15	8.152	0.019	0.037	4.565
VII	1st	Ct	Ct	Ct	9	7.814	7.851	7.833	7.828	0.029	0.037	4.626

Table 4. The bundle adjustment results of Image 3(Look angle: Left=-25.9 deg., Right=27.4 deg.) (Unit: m)

Case	Position	Attitude			Iter.	Covariance				Residual		RMSE
	X,Y,Z	ω	ϕ	κ		σ_X	σ_Y	σ_{XY}	σ_Z	V_X	V_Y	XYZ
I	1st	1st	1st	1st	13	3.901	3.922	3.912	3.906	0.022	0.031	5.109
II	1st	2nd	2nd	2nd	10	3.865	3.883	3.874	3.871	0.018	0.027	6.194
III	2nd	2nd	2nd	2nd	10	4.673	4.694	4.684	4.695	0.017	0.027	6.139
IV	1st	Ct	1st	1st	10	3.749	3.768	3.758	3.753	0.022	0.031	5.154
V	1st	Ct	Ct	1st	10	3.625	3.644	3.634	3.629	0.022	0.031	5.133
VI	1st	Ct	Ct	2nd	11	3.957	3.978	3.968	3.965	0.025	0.031	5.518
VII	1st	Ct	Ct	Ct	9	3.573	3.592	3.583	3.578	0.024	0.031	5.091

the performance of linear position models are better than the quadratic models.

As the orders of polynomial degrees increase, the adjusted ground coordinates of standard deviation also increase. That is, rather than the decrease of bundle adjustment precision, polynomial orders of exterior orientation increase and the weighting factors also increase.

As the tilt angle increase, the image coordinates residuals increase too. The conversion speed of bundle adjustment is unstable. In the process of bundle adjustment, most of the tests had been executed 10 times under. This shows the high speed of conversion iteration.

After bundle adjustment, by utilizing images of 3 different tilt angles, the results of sensor modeling are follows; The stereo pairs Daejeon I and Seoul II, the best case of adjusted parameters is Case VII with results the other 6 cases (Table 2).

Case VII is first degree of polynomials with ΔX, ΔY, ΔZ constant for $\Delta\omega$, $\Delta\phi$, $\Delta\kappa$ where average RMSE is 3.196 meters and 5.091 meters. In Seoul I stereo pair, the best case of adjusted parameters is case VI with results the other 6 cases.(Table 2)

Case VI is first degree of polynomials with ΔX, ΔY, ΔZ constant for $\Delta\omega$, $\Delta\phi$ and quadratic $\Delta\kappa$ where average RMSE is 4.565 meters.

By looking at the check point accuracy in Tables 2~4 the average RMSEs (3.196m, 4.565m, 5.091m) are all 1 pixel below of the KOMPSAT-1 EOC spatial resolution. This does not greatly influence the tilt angle. The change in the tilt angle does not increase the accuracy of ground object coordinates. The tilt angle effects two quality of image coordinates (column and line coordinate), since the image u-coordinates are especially sensitive, and the tilt rotates around the u-axis. For the v-coordinates, the tilt increase reduces the required error magnitude and the same is true for the combined case.

6. Conclusions

The effect of the tilt angle on the mathematical model are studied in this research. These are the steps taken for the tilting angles (5°, 15°, 25°) of KOMPSAT-1 for the evaluation of geometric accuracy of three different stereo images: Firstly, as the tilting angle is different in each image, the characteristic of satellite dynamic must be determined by sensor modeling. Then the best sensor modeling equation is determined. The best set of parameters are the 6 position deviation parameters (1st order polynomial) with 1 yaw angle or three yaw angle deviation parameters in addition. The change in the tilt angle does not increase the accuracy of the ground object coordinates. The tilt angle effects two quality of image coordinates, especially since the image u-coordinates are sensitive.

Reference

1. Chen, L. C. (1993), "Rigorous generation of digital orthphotos from SPOT images", PE&RS, ASPRS, Vol. 59, No. 5, pp. 655-661.[Journal]
2. Fritsch, D. and Stallmann, D. (2000), "Rigorous Photogrammetric Processing of High Resolution Satellite Imagery", IAPRS, Vol. XXXIII, Part B1, Amsterdam 2000, pp. 313-321. [Proceeding]
3. Makki, S. H. (1991), Photogrammetric reduction and analysis of real and simulated SPOT imageries, Purdue University, A thesis of Purdue University, pp. 17-45.[Thesis]
4. Mikhail E. M. and Bethel J. S. (2001), Introduction to Modern Photogrammetry, New York, John Wiley and Sons Ins. [Book]
5. Westin, T. (1990), "Precision Rectification of SPOT Imagery", PE&RS, ASPRS, Vol. 56, No. 2, pp. 247-253.[Journal]
6. Korea Aerospace Research Institute http://www.kari.re.kr, 2003. 7. 24[Web page]